

Observation of Weak Localization of Light in a Finite Slab: Anisotropy Effects and Light-Path Classification

Meint P. van Albada, Martin B. van der Mark, and Ad Lagendijk

Natuurkundig Laboratorium, Universiteit van Amsterdam, NL-1018 XE Amsterdam, The Netherlands

(Received 13 August 1986)

We report on the dependence of enhanced backscattering of light in a random medium on sample thickness, mean free path, and size of scattering centers. Introduction of a new difference technique allows for independent observation of contributions from long and short light paths in a suspension of polystyrene spheres. A *new* anisotropy effect, which has been found to be most prominent for the smallest particles studied, could be classified as a lower-order multiple-scattering phenomenon.

PACS numbers: 42.20.-y, 71.55.Jv

Recently a precursor of Anderson localization of light,¹⁻⁴ referred to as weak localization, has been observed.^{5,6} The onset of localization manifests itself in the form of a narrow cone of enhanced backscattering from random media.⁷ The detection of Anderson localization of light most likely will involve the monitoring of (angular resolved) transmission and/or backscattering. In both cases the dependence on sample thickness will be a crucial factor in such an experiment. For this reason it is essential to understand the interference effects in the propagation of light in random media of *finite* thickness.

In this work we report on the results of an extensive study of the phenomenon of weak localization of light in a *finite* slab. Our samples consist of concentrated suspensions of polystyrene spheres. In studying the enhanced backscattering we varied the thickness of the sample, particle size, concentration of the suspension, and spatial orientation of the scan with respect to the plane of polarization of the incident beam. Observing the dependence of weak localization on these parameters we have found a new anisotropy effect which, by employing a difference technique, could be attributed to lower-order (mainly second-order) multiple scattering. From the theoretical side we have solved rigorously the summation of most-crossed diagrams for isotropic scalar point scatterers for a *finite* slab. The new theory is compared with the results of experiments in which incident and detected polarization are parallel. Agreement is good as long as the newly found anisotropy effect is unimportant, that is, for suspensions of all but the smallest particles studied. The anisotropy effect, that depends crucially on the vector character of light, will be explained qualitatively.

Our experimental setup is a sophisticated extension of our earlier equipment.⁵ Resolution is about 0.4 mrad. Routinely, scans have been performed parallel and perpendicular to the direction of the incoming polarization, alternatively with a parallel or a crossed polarizer in front of the detector.

In the measured intensity in the 180° direction, the contribution of most-crossed diagrams corresponds to in-

terference between light paths and their time-reversed counterparts. For *scalar* waves, this interference will result in an enhancement factor of 2 for *multiple* scattering. (The *total* enhancement factor will be <2 if the *single*-scattering contribution is nonnegligible.) For *vector* waves, the outgoing polarization vectors for mutually time-reversed paths can be represented by $\mathbf{p}_{\text{out}}^+ = \mathbf{M} \cdot \mathbf{p}_{\text{in}}$ and $\mathbf{p}_{\text{out}}^- = \bar{\mathbf{M}} \cdot \mathbf{p}_{\text{in}}$, where $\bar{\mathbf{M}}$ is the transpose of \mathbf{M} . Choosing $(\hat{\rho})$ as the incoming polarization vector, the parallel and perpendicular intensities in the 180° direction relate as $\langle (2M_{11})^2 \rangle$ and $\langle M_{12}^2 \rangle + \langle M_{21}^2 \rangle + 2\langle M_{12} \times M_{21} \rangle$, where brackets represent averaging over all light paths. So, for the parallel component the enhancement factor is always 2, whereas for the perpendicular component it depends on $\langle M_{12}M_{21} \rangle$. For second-order scattering $M_{12} = M_{21}$, and the perpendicular enhancement factor is 2. For increasing order, $\langle M_{12}M_{21} \rangle$ rapidly decreases, and the perpendicular enhancement factor converges towards 1.⁸ For second-order Rayleigh scattering $\langle M_{11}^2 \rangle = 8\langle M_{12}^2 \rangle$ (partial retention of polarization). For higher order $\langle M_{12}^2 \rangle / \langle M_{11}^2 \rangle$ rapidly converges towards 1 (complete depolarization).

For *isotropic* (scalar) scattering the relative contributions of different-order processes to the total incoherent backscattering can be calculated from Milne theory.⁹ From a slab of optical thickness 1 ($d = \lambda_{\text{mf}}$), 40% of the intensity in the 180° direction comes from first-order scattering, and 36% from combined second and third order. For a semi-infinite slab these percentages are still 12 and 16, respectively. Since we are dealing with *vector* waves, isotropic scattering does not apply. In *anisotropic* scattering, the relative contributions of the orders to backscattering will depend on the scattering matrix of the particles. For Rayleigh scattering we expect the "lower-order" contributions to be of the same order of magnitude as for the isotropic case (cf. Ref. 9 for a quantitative confirmation). For Mie scattering we expect them to decrease with increasing particle size, but not by many orders of magnitude. We conclude that scattering processes that contribute to backscattering with a (partial) retention of polarization and with a per-

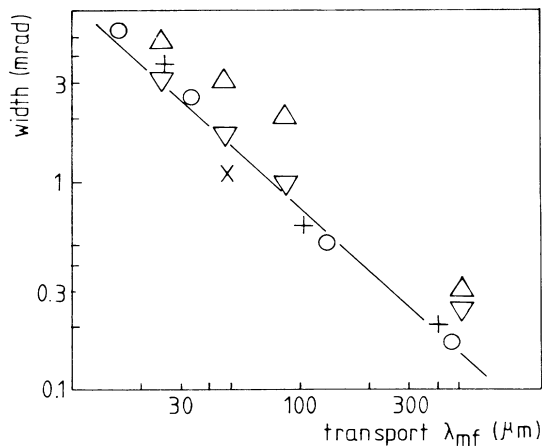


FIG. 1. Width of the cone backscattered from suspensions in water (not corrected for refraction at the interface) as measured at 1.5 times the background level vs transport λ_{mf} as calculated from Mie theory. Background of the 0.215- μm particle suspensions has been corrected for the single-scattering contribution. Symbols: crosses represent 2.02- μm polyvinyltoluene; open circles represent 1.091- μm polystyrene; pluses represent 0.482- μm polystyrene; inverted triangles represent 0.215- μm polystyrene, spatial scan perpendicular to polarization vector; triangles represent 0.215- μm polystyrene, spatial scan parallel to polarization vector. Solid line. $\text{FWHM} = 0.72\lambda_{vac}/2\pi\lambda_{mf}$.

pendicular enhancement factor > 1 may participate to a measurable extent in all the samples studied. We refer to these processes as lower-order processes.

On the basis of simple scaling theory, one predicts for semi-infinite slabs enhanced backscattering within an (full) apex angle $\sim \lambda/(2\pi\lambda_{mf})$ (λ_{mf} is the transport mean free path for light of wavelength λ in the medium). Since the backscattered light contains low-order contributions, which are sensitive to details of the single-particle scattering matrix, the shape of the cone is expected to depend somewhat on the nature of the scattering particles. So one expects the width of the cone to be proportional to λ/λ_{mf} , hopefully with a proportionality constant weakly dependent on the detailed scattering matrix. This hypothesis is found to hold quite well (cf. Fig. 1).

The two sets of data for 0.215- μm particle suspensions obtained from scans in which the detector was moved parallel to the incoming polarization and perpendicular to it respectively, lie on different lines; i.e., the corresponding "cones" are actually elliptically shaped [cf. Fig. 2(a)]. This can be explained qualitatively as follows: Consider two planes through the direction of incidence, one perpendicular to the incident polarization vector, the other including this vector. A small particle will scatter more power into directions included in the former plane than in the latter. If low-order scattering is important,

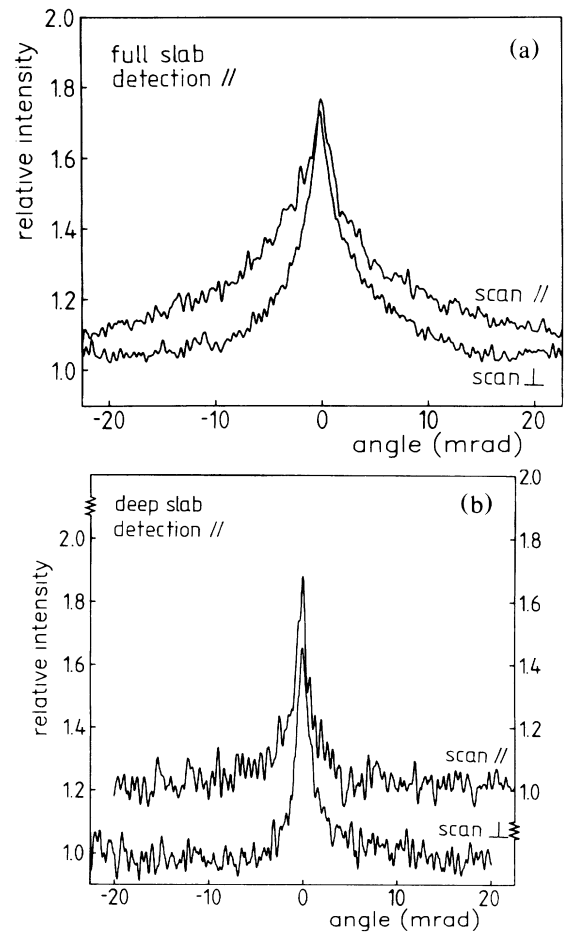


FIG. 2. (a) Total backscattering cone from a 1500- μm slab of 9.6 vol% of 0.215- μm polystyrene particles in water as a function of angle. Upper curve: spatial scan parallel to polarization vector; lower curve: spatial scan perpendicular to polarization vector. The two curves differ approximately by a factor of 2 in width. (b) Difference backscatter cones from the slab between 60 and 1500 μm of the suspension of (a). The mutually perpendicular scans now give the same width [compare (a)].

light paths having both ends in or near planes perpendicular to the polarization vector will be relatively favored. Interference between waves emerging from these ends will be less sensitive towards a displacement of the detector parallel to the polarization vector than towards one in the perpendicular direction.

The state of polarization of the enhanced backscatter cone and of the background has been carefully studied as a function of particle size and sample thickness. In Table I we present part of our results. Enhancement factors are defined as the ratio of total backscattering at exactly 180° and background. It is seen that upon going from thin slabs to thick slabs (1) the parallel enhance-

TABLE I. Enhancement factors and polarization characteristics of the background for various values of particle size and slab thickness. The samples are 9.6-vol% suspensions.

Size (μm) [λ_{mf} (μm)] ^a	Thickness sample (μm)	Enhancement		I_{\parallel}/I_{\perp} ^b background
		\parallel	\perp	
1.091 (34)	10	1.17	1.19	1.86
	40	1.50	1.39	1.19
	125	1.62	1.29	1.07
	500	1.66	1.20	1.03
	1500	1.65	1.22	1.05
0.482 (25)	40	1.55	1.29	1.26
	250	1.59	1.17	1.16
	1500	1.66	1.13	1.09
0.215 (25)	50	1.44	1.19	2.74
	100	1.51	1.18	2.12
	200	1.48	1.12	1.86
	800	1.49	1.11	1.70
	2500	1.51	1.11	1.60

^aTransport mean free path.

^b I_{\parallel} including single scattering.

ment factor increases (reflecting a decreasing relative importance of single scattering), (2) the perpendicular enhancement factor decreases (reflecting a decreasing relative importance of lower-order multiple scattering), and (3) the depolarization of the background becomes more complete (reflecting a decreasing relative importance of single and low-order multiple scattering). Apparently, low-order processes play an important part. For several reasons one would like to separate out these lower-order contributions. In the first place localization is concerned with the long light paths (long in terms of the mean free path). Furthermore, for longer light paths scattering is more likely to be well described by a simple and universal model of isotropic scattering. We have developed the following method for probing the contribution of exclusively higher-order scattering (long light paths): Taking the difference between the backscattering patterns of slabs of thickness L_1 and L_2 ($L_2 > L_1$), the low-order scattering contributions coming from the front layer of the sample ($L < L_1$) cancel out, and what remains is the contribution of light that has "seen" the deeper part of the slab ($L_1 < L < L_2$).

"Difference cones" from the slab between 60 and 1500 μm of a 9.6-vol% suspension of 0.215- μm polystyrene spheres are shown in Fig. 2(b). The curves labeled \parallel and \perp have been obtained from spatial scans parallel and perpendicular to the direction of polarization of the incident beam. In both cases the component polarized parallel to the incident beam was recorded. In contrast to the "complete" cones given in Fig. 2(a), these difference cones are equally wide, showing that the very broad anisotropic contribution to the complete cone in the parallel scan is a low-order multiple-scattering effect coming from the very front layer of the sample.

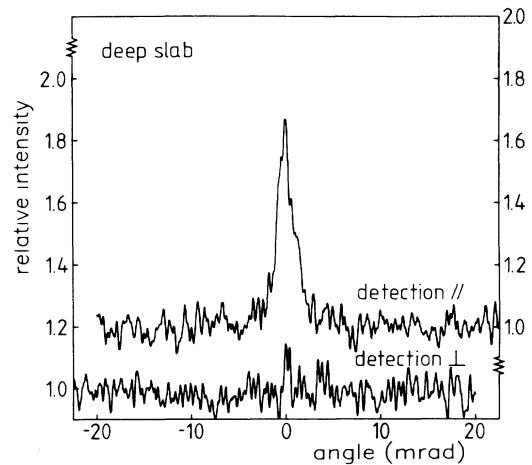


FIG. 3. Parallel and perpendicularly polarized difference in critical backscattering from the slab between 70 and 1500 μm of 9.6 vol% of 1.091- μm polystyrene in water. Upper curve: detected light polarized parallel to incident light. Lower curve: detected light polarized perpendicular to incident light.

The difference cones in Fig. 3 originate from the slab between 70 μm and 1500 μm of a 9.6 vol% suspension of 1.091- μm particles. The upper curve shows the cone for the light component polarized parallel to the incident beam. In the top, an enhancement factor of 1.7 (limited by experimental resolution) was found. The lower curve shows the difference pattern for the perpendicularly po-

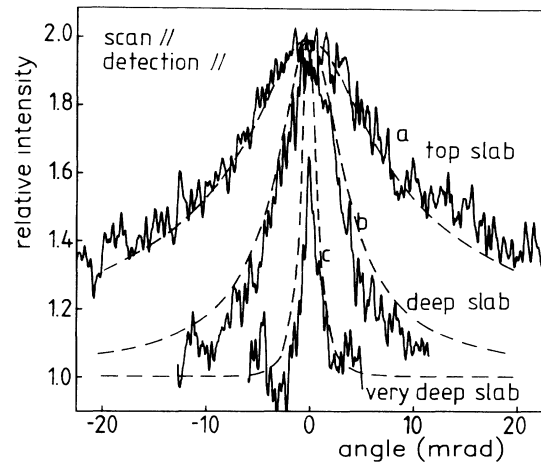


FIG. 4. Experimental cone shapes from a 9.6-vol% 0.482- μm particle suspension. Curve *a* corresponds to a slab thickness of 15 μm , curve *b* corresponds to the 45- μm -15- μm , and curve *c* corresponds to the 1500- μm -70- μm difference scattering. Curve *c* is resolution limited. The FWHM of the absolute scan (not shown here) is 3.7 mrad, and the enhancement factor is 1.8. All results refer to parallel-polarized backscatter (detected light has the same polarization as the incoming laser beam). Dashed lines: theoretical curves.

larized component. Here no cone is seen at all, whereas in an absolute scan (including the first 70 μm of the slab) a clear perpendicularly polarized cone with an enhancement factor of 1.2 can be observed. Clearly, the perpendicularly polarized cone results from low-order scattering contributions.

Upon moving away from the 180° direction one expects the longer light paths to get out of phase earlier than the short light paths. Consequently, the long light paths should yield narrower contributions to the cone of enhanced backscattering. This is beautifully demonstrated in the experimental results depicted in Fig. 4. This figure shows the *shapes* of contributions to the cone from a 1500- μm slab of a 9.6-vol% suspension of 0.482- μm particles, originating from one "full" slab and two "difference" slabs. All cones are normalized with respect to their own multiple-scattering background (which for the 0-15- μm full cone means a substantial correction for first-order scattering). It is seen that after elimination of the single-scattering contribution the enhancement factor for the parallel light component is near 2 (curves *a* and *b*) until the limit of experimental resolution is reached (curve *c*).

If one uses isotropic (scalar) scattering by point particles as a model for the parallel-polarized backscattering, one can sum the most important scattering diagrams for interference (the most-crossed diagrams) rigorously for a finite slab. The resulting equation for the interference contribution is very analogous to the Milne equation⁹ for the incoherent part of the multiple scattering.^{7,10} These equations are, of course, most difficult to solve for the conservative case (albedo=1), which is most relevant for

our experiments, and become rather trivial for albedo slightly smaller than 1. We have solved these equations rigorously by diagonalization but we have also sampled the contributions order by order.¹⁰ The theoretical cones indeed follow the expected behavior: Each higher order has a narrower cone. For all particle sizes studied except for the smallest the theory gives good results (cf. Fig. 4). For thick slabs the resulting theoretical FWHM is $0.72\lambda/(2\pi\lambda_{mf})$, remarkably close to the experimental result (cf. Fig. 1).

This work is part of the research program of the Stichting voor Fundamenteel Onderzoek der Materie (FOM), which is financially supported by the Nederlandse Organisatie voor Zuiver-Wetenschappelijk Onderzoek (ZWO).

¹S. John and M. J. Stephen, Phys. Rev. B **28**, 6358 (1983).

²S. John, Phys. Rev. Lett. **53**, 2169 (1984).

³T. R. Kirkpatrick, Phys. Rev. B **31**, 5746 (1985).

⁴E. Akkermans and R. Maynard, J. Phys. (Paris), Lett. **46**, L1045 (1985).

⁵M. P. van Albada and A. Lagendijk, Phys. Rev. Lett. **55**, 2692 (1985).

⁶P. E. Wolf and G. Maret, Phys. Rev. Lett. **55**, 2696 (1985).

⁷L. Tsang and A. Ishimaru, J. Opt. Soc. Am. A **2**, 2187 (1985).

⁸The full solution for the perpendicular cone in Rayleigh scattering has been given very recently: M. J. Stephen and G. Cwillich, to be published.

⁹H. C. van de Hulst, *Multiple Light Scattering* (Academic, New York, 1980), Vols. I and II.

¹⁰Details of the theory will be published elsewhere.